Inorganic Chemistry

Article

pubs.acs.org/IC

Linear Coordination Fullerene C_{60} Polymer $[\{Ni(Me_3P)_2\}(\mu\text{-}\eta^2,\eta^2\text{-}C_{60})]_\infty$ Bridged by Zerovalent Nickel Atoms

Dmitri V. Konarev,*[,†] Salavat S. Khasanov,[§] Yoshiaki Nakano,[‡] Akihiro Otsuka,[‡] Hideki Yamochi,[‡] Gunzi Saito,[∥] and Rimma N. Lyubovskaya[†]

[†]Institute of Problems of Chemical Physics and [§]Institute of Solid State Physics, Russian Academy of Sciences , Chernogolovka, Moscow 142432, Russia

[‡]Research Center for Low Temperature and Materials Sciences, Kyoto University, Sakyo-ku, Kyoto 606-8501, Japan

[∥]Faculty of Agriculture, Meijo University, 1-501 Shiogamaguchi, Tempaku-ku, Nagoya 468-8502, Japan

Supporting Information

ABSTRACT: Coordination nickel-bridged fullerene polymer $[\{Ni(Me_3P)_2\}(\mu\text{-}\eta^2,\eta^2\text{-}C_{60})]_\infty$ (**1**) has been obtained via reduction of a $Ni^{II}(Me_3P)_2Cl_2$ and C_{60} mixture. Each nickel atom is linked in the polymer with two fullerene units by η^2-type Ni−C(C_{60}) bonds of 2.087(8)−2.149(8) Å length. Nickel atoms are coordinated to the 6−6 bonds of C_{60} as well as two trimethylphosphine ligands to form a four-coordinated environment around the metal centers. Fullerene cages approach very close to each other in the polymer with a 9.693(3) Å interfullerene center-to-center distance, and two short interfullerene C−C contacts of 2.923(7) Å length are formed. Polymer chains are densely packed in a crystal with interfullerene center-to-center distances between fullerenes from neighboring polymer chains of 9.933(3) Å and multiple interfullerene C···C contacts. As a result, three-dimensional dense fullerene packing is formed in **1**. According to optical and electron paramagnetic resonance spectra, fullerenes are neutral in **1** and nickel atoms have a zerovalent state with a diamagnetic d^{10} electron configuration. The density functional theory calculations prove the diamagnetic state of the polymer with a singlet−triplet gap wider than 1.37 eV.

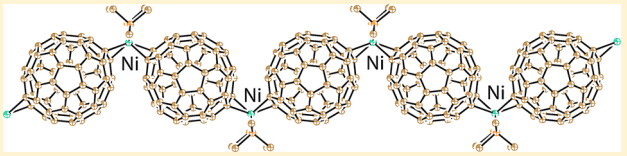

INTRODUCTION

Fullerene C_{60} forms a variety of transition-metal complexes with palladium, platinum, rhodium, ruthenium, osmium, nickel, cobalt, and some other metals, which coordinate to the 6−6 fullerene bonds.[1] Such complexes can show promising magnetic and conducting properties when paramagnetic transition metals are used or charge is partially transferred from the metal centers to fullerenes. Of special interest in the design of metal−fullerene complexes are dimeric or polymeric structures because close distances between the metal centers and fullerene cages can provide strong magnetic coupling of spins or movement of electrons along the polymeric chains. However, most of the obtained transition metal−fullerene complexes have monomeric fullerene units with coordination of one[1] or even several metal centers[2] to one fullerene cage. Several dimers are known in which two fullerene cages are bridged by zerovalent molybdenum, tungsten, cobalt, or nickel atoms.[3] The Ir_4 and Rh_6 clusters can also bind two fullerene cages to form the dimeric structure.[4] In most cases, interfullerene distances are rather long in metal-bridged fullerene dimers. Short interfullerene center-to-center (ctc) distances and short distances between the metal centers are observed in the $\{Co(Ph_3P)(C_6H_5CN)\}_2(\mu\text{-}\eta^2,\eta^2\text{-}C_{60})_2$ and $\{Ni(Ph_3P)\}_2(\mu\text{-}\eta^2,\eta^2\text{-}C_{60})_2$ dimers only.[3b,c] In these cases, a cobalt−fullerene dimer with paramagnetic Co^0 centers ($S = {}^1/_2$) has an excited triplet state at high temperatures with strong exchange interaction between spins localized on the cobalt atoms ($J/k_B = -28.6$ K), and a transition to a diamagnetic singlet ground state occurs below 35 K.[3b]

Metal-bridged fullerene polymers are also known.[5] They were obtained chemically by adding labile platinum or palladium complexes to C_{60}[5a−c] or electrochemically.[5d−h] These polymers have the composition $C_{60}Pt$ (or $Pd)_x$, where $x = 1-7$. It is believed that a compound of the composition $C_{60}M_1$ is a one-dimensional polymer with alternating metal atoms and C_{60} cages in the chains. Polymers with higher metal content can even contain cross-links formed by metal atoms between neighboring fullerene chains.[5a−c] Insoluble europium-bridged polymers of the composition $C_{60}Eu_x$ ($x = 1-6$) are also known.[5i] However, crystalline compounds with such polymers have not been obtained so far, and hence their crystal structures are still unknown.

Previously, we had developed a method for the preparation of transition metal−fullerene complexes by the reduction of $Co^{II}(Ph_3P)_2Br_2$ or $M^{II}(L)Cl_2$ [M = Ni, Co; L = 1,2-bis(diphenylphosphino)ethane, 1,3-bis(diphenylphosphino)-propane, 1,1′-bis(diphenylphosphino)ferrocene] and fullerene mixtures by different reductants such as sodium fluorenone ketyl, sodium tetraphenylborate, or zinc dust. This allows one to obtain a series of nickel- and cobalt-containing monomeric and dimeric fullerene complexes.[3b,c,6] In this work, we found

Received: June 30, 2014
Published: November 4, 2014

   dx.doi.org/10.1021/ic501551y | Inorg. Chem. 2014, 53, 11960−11965

that when $Ni^{II}(Me_3P)_2Cl_2$ with a small ligand of trimethylphosphine is used for the preparation of a complex with fullerene, the $Ni(Me_3P)_2$ fragment coordinates to two fullerene cages, providing the formation of infinite polymeric $[\{Ni(Me_3P)_2\}(\mu\text{-}\eta^2,\eta^2\text{-}C_{60})]_\infty$ (**1**) chains. We for the first time present the molecular structure and optical and magnetic properties of a nickel–fullerene polymer. Theoretical calculations allow the electronic structure of this polymer to be elucidated. The developed approach should open a way to prepare polymeric transition metal–fullerene complexes, which show promising physical properties.

RESULTS AND DISCUSSION

Synthesis. **1** was obtained by the reduction of a stoichiometric mixture of $Ni^{II}(Me_3P)_2Cl_2$ (Aldrich) and C_{60} by an excess of zinc dust in *o*-dichlorobenzene for 10 min at 160 °C. The solution was cooled to room temperature. Then 0.1 mL of *N*,*N*-dimethylformamide (DMF) was added, and the reaction mixture was stirred for 24 h to produce a green solution. A similar procedure was also carried out with 0.1 mL of benzonitrile which was added as the coordinating polar solvent instead of DMF. Crystals of **1** were precipitated over 1 month by slow mixing of the obtained solution with *n*-hexane. In both cases, needlelike crystals formed were isostructural to each other according to the X-ray diffraction data. Platelike crystals also formed in low yield in the synthesis with DMF together with the needlelike crystals. Examination of the platelike crystals showed that they are isostructural to the needlelike crystals. The composition of **1** was determined from X-ray diffraction on single crystals. All tested crystals belong to one crystal phase. Zinc dust is a suitable reductant for both $Ni^{II}(Me_3P)_2Cl_2$ and C_{60} because of a negative enough standard electrode potential (−0.76 V). We found experimentally that zinc can generate $C_{60}^{\bullet-}$ in the presence of organic cations in pure *o*-dichlorobenzene. This reduction can produce even C_{60}^{2-} dianions in polar solvents like DMF.[7] However, the reduction is most probably centered on $Ni^{II}(Me_3P)_2Cl_2$ in the absence of organic cations. The generation of a green solution is also possible in pure *o*-dichlorobenzene. However, in this case, a black powder was formed over 1 day probably because of precipitation of a powdered coordination polymer. Most probably, the role of polar-coordinating solvent molecules in the synthesis of **1** is their coordination to nickel atoms to hinder polymerization. However, they are slowly substituted by fullerenes when polymer **1** is formed.

Spectra in the IR and UV–Visible–Near-IR (NIR) Ranges. IR spectra of **1** and starting $Ni^{II}(Me_3P)_2Cl_2$ are shown in the Supporting Information (SI; Table S1 and Figure S1). Four IR-active modes of C_{60} appear at 505, 520, 529, 579, 1184, 1416, and 1422 cm^{-1}. It is seen that the $F_{1u}(1)$ mode of starting C_{60} at 526 cm^{-1} is split into three bands at 505, 520, and 529 cm^{-1} because of the symmetry lowering of C_{60} stemming from the coordination of nickel. The $F_{1u}(4)$ mode sensitive to charge transfer to a fullerene molecule[8] is shifted from 1429 cm^{-1} (starting C_{60}) to 1416 and 1422 cm^{-1}. This shift can be due to weak π-back-donation.[1a] The UV–visible–NIR spectrum of **1** is shown in Figure 1. The bands at 260 and 335 nm can be attributed to intramolecular transitions in fullerene C_{60}, whereas the band with the approximate maximum at 700 nm is due to charge transfer between the metal and fullerene units. The latter band is very broad and shows absorption up to 1100 nm (Figure 1). No additional bands with maxima at 940–960 and 1070–1080 nm attributed $C_{60}^{\bullet-}$[9] in the spectrum of **1** indicate the absence of charge transfer from nickel atoms to the fullerene cage. Therefore, nickel atoms have a zerovalent state in **1** like in other known nickel–fullerene complexes.[3c,6a,c]

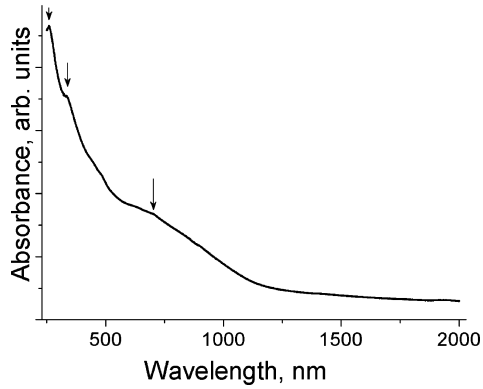

Figure 1. UV–vis–NIR Spectrum of **1** in the 250–2000 nm range in KBr pellets prepared under anaerobic conditions.

Crystal Structure. The crystal structure of **1** was determined at 280 and 100 K. Views of the nickel–fullerene coordination polymer at 280 K along the *c* and *a* axes are shown in Figure 2a,b. There is one crystallographically independent half of the C_{60} molecule at 280 K, which is disordered between two orientations with 0.608(5)/0.392(5) occupancies. Each nickel atom is bound with two fullerene units by the η^2-type $Ni–C(C_{60})$ bonds in both orientations. The lengths of these bonds are 2.107(1) and 2.132(1) Å for major and 2.121(1) and 2.116(1) Å for minor fullerene orientations. Such a type of disorder is not usual for transition metal–fullerene complexes in which metal coordination completely orders fullerene cages.[1−5] Coordination is realized by oppositely located shorter 6–6 bonds of C_{60} in both orientations (ring junction between two hexagons). These 6–6 bonds are elongated up to 1.449(6)–1.450(6) Å at 280 K (Figure 3) in comparison with the average length of other 6–6 bonds in C_{60} [1.385(8) Å]. The longer 6–5 bonds with carbon atoms involved in coordination with nickel atoms are also elongated up to 1.472(10)–1.473(10) Å compared with the average value of 1.451(9) Å. The elongation of the 6–6 bonds found previously in some transition-metal C_{60} complexes was attributed to π-back-donation.[1a] As a result of nickel coordination, the C_{60} cage is elongated by 0.30–0.33 Å along the *a* axis in comparison with the distances in two other perpendicular directions. Nickel atoms also coordinate two trimethylphosphine ligands, which together with fullerenes form a four-coordinated environment around the metal centers. Then the geometry is distorted tetrahedral. Namely, the ability of nickel atoms in $Ni(Me_3P)_2$ to form a distorted tetrahedral environment provides the formation of a coordination polymer in **1**. The range of C–Ni–C and P–Ni–P angles is 100.6–121° at 280 K (Figure 3). The $Ni–P(Me_3P)$ bonds in **1** are 2.286(1) Å length. Previously, it was found that the Ni(L) fragments with bulky ligands have a nearly square-planar coordination environment for nickel atoms. In this case, both $Ni–C(C_{60})$ and Ni–P(L) bonds are essentially shorter and positioned in the 1.933(6)–1.987(3) and 2.130(2)–2.210(1) Å ranges, respectively.[6a−c] The shortest Ni···Ni distance between the polymer chains was found to be 9.933(6) Å, whereas this distance within the polymer chain is slightly longer at 11.230(6) Å.

dx.doi.org/10.1021/ic501551y | Inorg. Chem. 2014, 53, 11960–11965

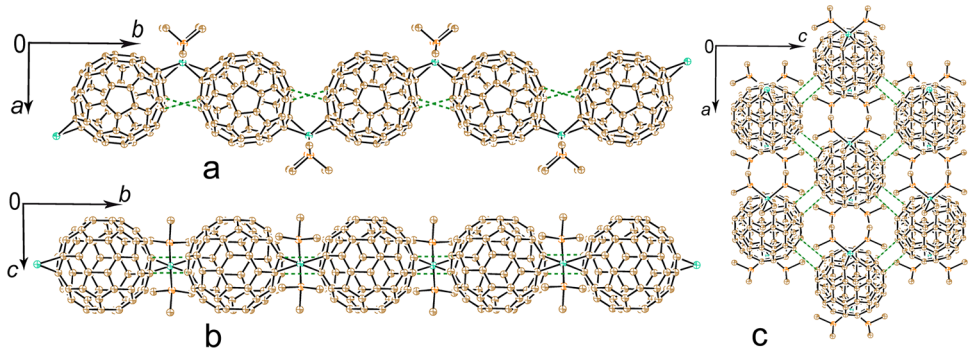

Figure 2. Structure of the nickel–fullerene polymeric chain in **1** at 280 K viewed along the *c* and *a* axes (a and b, respectively). View of the crystal structure of **1** along the polymeric chains and the *b* axis (c). Short vdW interfullerene C···C contacts are shown by green dashed lines. Only the major orientation of C_{60} is shown.

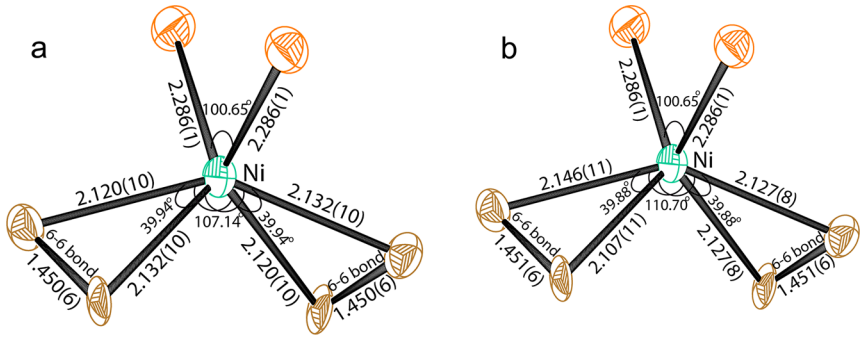

Figure 3. Two types of coordination surrounding for nickel atoms in the major (a) and minor (b) orientations of C_{60} at 280 K.

The bonding of two fullerenes by nickel with rather short Ni–C(C_{60}) bonds results in a very close approach of fullerene cages to each other in the polymer with only 9.693(3) Å interfullerene ctc distances and the formation of two short C–C contacts between fullerenes of 2.923(7) Å. Nevertheless, a 2 + 2 cycloaddition reaction between fullerenes[10] does not take place. Generally, ctc interfullerene distances and van der Waals (vdW) interfullerene C···C contacts in molecular and ionic fullerene solids with closely packed one-dimensional C_{60} chains are noticeably longer (>9.91–9.92 and >3.08–3.37 Å, respectively).[11] Polymer chains are also closely packed in a crystal with an interfullerene ctc distance between fullerenes from neighboring polymer chains of 9.933(3) Å (each C_{60} has four such neighbors; Figure 2c). The distance of 9.933(3) Å is essentially shorter than the vdW diameter of C_{60} (10.18 Å), allowing the formation of eight vdW C···C contacts of 3.19 Å length for each C_{60}. As a result, dense three-dimensional packing of fullerenes is formed in **1** in which each C_{60} has six fullerene neighbors at 9.7–9.9 Å ctc distances. These distances in a pure C_{60} or three-dimensional $C_{60}{\cdot}C_2H_4$ solid are 10.02–10.04 Å, but the number of fullerene neighbors for each C_{60} is 12.[12]

The appearance of new weak superstructural reflections below 280 K indicates a structural transition from an orthorhombic to a monoclinic lattice with doubling of the unit cell volume because of translational symmetry changes in the *ac* plane, i.e., perpendicular to the chain axis. The structure at 100 K has two crystallographically independent building units for one-dimensional chains, with the building units each a centered nickel core with two Me_3P ligands and two halves of C_{60}. Although a structural transition is realized most probably because of fullerene ordering, they are still disordered between two orientations even at 100 K. However, they do not have equal occupancies, namely, 0.631(6)/0.369(6), 0.598(9)/0.402(9), 0.741(5)/0.259(5), and 0.888(4)/0.112(4), at 100 K. This is the difference from the high-temperature phase, where the occupancies were detected to be 0.608(5)/0.392(5) at 280 K. It seems that there are no specific interactions that can provide this ordering, but it could be "normal" low-temperature ordering, as is observed in pure fullerite.[13] The length of the Ni–C(C_{60}) contacts at 100 K is 2.095(5)–2.140(5) Å, the ctc interfullerene distance in the polymer is 9.675(2) Å (nearly the same as that at 280 K), and the distance between fullerenes from the neighboring polymeric chains is 9.881(2) Å. The shortest Ni···Ni distance between the polymer chains decreases to 9.783(6) Å at 100 K.

Magnetic Properties. SQUID and electron paramagnetic resonance (EPR) measurements showed that **1** is diamagnetic in the 300–1.9 K range) and EPR-silent at room temperature. This is in agreement with the absence of charge transfer from nickel to fullerene concluded from optical spectra and indicates a diamagnetic d^{10} electron configuration for nickel(0) atoms. All previously studied monomeric and dimeric fullerene C_{60} complexes with nickel(0) also show the absence of charge transfer to the fullerene cage and a diamagnetic d^{10} electron configuration for the nickel(0) atoms.[3c,6a,c]

Calculations. The electronic structure of the nickel-bridged C_{60} polymer in **1** was examined using theoretical analysis based on density functional theory (DFT) and oligomer models of $\{Ni(Me_3P)_2\}(C_{60})_2$, $\{Ni(Me_3P)_2\}_2(C_{60})_3$, $\{Ni(Me_3P)_2\}_3(C_{60})_4$, and $\{Ni(Me_3P)_2\}_4(C_{60})_5$ determined from X-ray analysis (Figure 2). Singlet and triplet states were investigated at the CAM-B3LYP/LanL2DZ/6-31G(d,p) level of theory. The total and relative energies and $\langle S^2 \rangle$ values are shown in Table S2 in

dx.doi.org/10.1021/ic501551y | *Inorg. Chem.* 2014, 53, 11960–11965

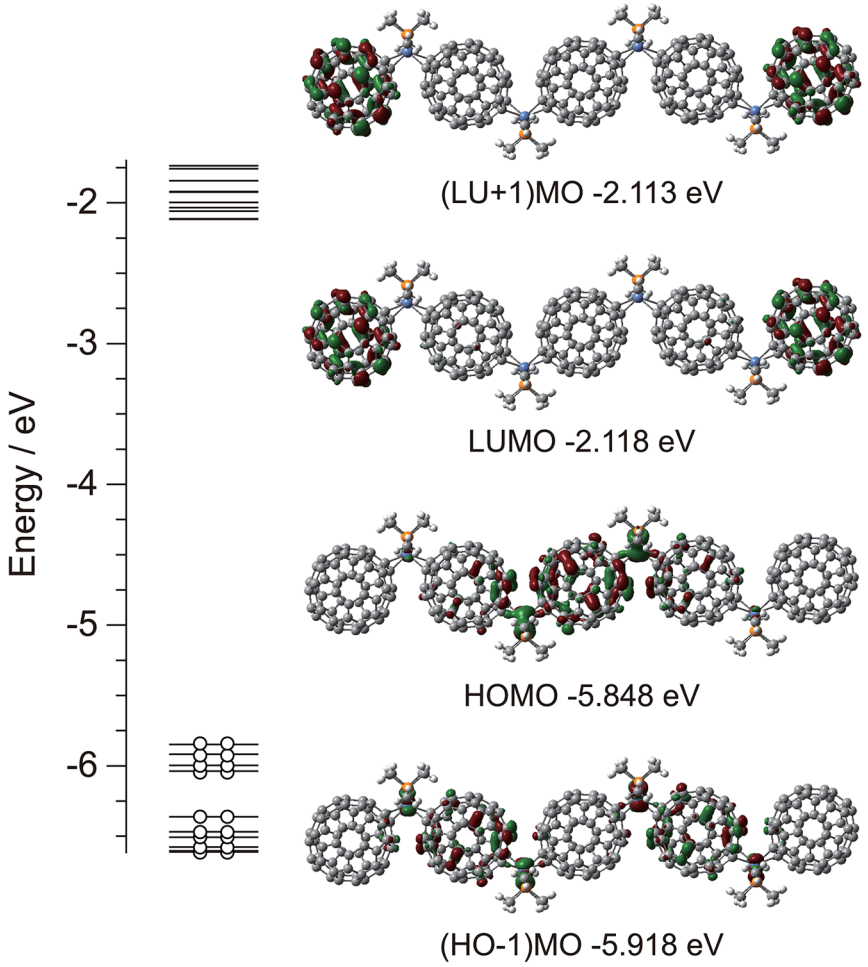

Figure 4. Energy diagram of frontier Kohn–Sham orbitals for the ^1A_g state of $\{Ni(Me_3P)_2\}_4(C_{60})_5$ calculated at the RCAM-B3LYP/LanL2DZ/6-31G(d,p) level of theory.

the SI. As derived from the $\langle S^2 \rangle$ values, the spin contamination is nearly negligible for the calculated triplet states since the $\langle S^2 \rangle$ values close to 2 correspond to the pure triplet state. In the calculated oligomers of $\{Ni(Me_3P)_2\}(C_{60})_2$, $\{Ni(Me_3P)_2\}_2(C_{60})_3$, $\{Ni(Me_3P)_2\}_3(C_{60})_4$, and $\{Ni(Me_3P)_2\}_4(C_{60})_5$, a comparison of the calculated total energies indicates that the closed-shell singlet states are much more stable energetically than the corresponding triplet states (singlet–triplet gap of more than 1.37 eV; Table S2 in the SI), which must be thermally inaccessible. Theoretical analysis supports the diamagnetic feature of polymer **1**. The energy diagram of frontier Kohn–Sham orbitals for the ^1A_g state of $\{Ni(Me_3P)_2\}_4(C_{60})_5$ is shown in Figure 4. The highest occupied molecular orbital is located around the nickel and phosphorus atoms of the inner $\{Ni(Me_3P)_2\}$ units and the central C_{60} molecule, whereas the lowest unoccupied molecular orbital (LUMO) and (LU+1)MO are nearly degenerate and are localized mainly on the outer C_{60} molecules. The calculated Mulliken and natural charges of nickel, Me_3P, and C_{60} molecules are shown in Tables S3 and S4 in the SI, respectively. The average charges of nickel and Me_3P were independent of the calculated oligomer models, where Mulliken [natural] charges of nickel and Me_3P were −0.55 [−0.23] and 0.38–0.39 [0.40], respectively. However, those of C_{60} were heavily dependent on the model, where Mulliken [natural] charges were −0.11 to −0.17 [−0.29 to −0.46]. The average charges of C_{60} [$\rho_{av}(C_{60})$] versus x/y plots in $\{Ni(Me_3P)_2\}_x(C_{60})_y$ oligomers are shown in Figure S3 in the SI. The $\rho_{av}(C_{60})$ versus x/y plot afforded the linear relationships of $\rho_{av}(C_{60}) = -0.1992(x/y) - 0.0129$ and $\rho_{av}(C_{60}) = -0.5635(x/y) - 0.0086$ for Mulliken and natural charges, respectively. Upon extrapolation of the data at $x/y = 1$, the Mulliken and natural charges of C_{60} were estimated as −0.21 and −0.57 in $[\{Ni(Me_3P)_2\}(C_{60})]_\infty$, respectively. The electron density slightly flows from the electron-donating Me_3P to C_{60} through the nickel atom. Although the charge of C_{60} was estimated more ionically, natural population analysis would afford a reasonable charge qualitatively. Theoretical analysis indicates that Me_3P is slightly positively charged, C_{60} is slightly negatively charged, and nickel is nearly neutral, which supports the experimental results.

■ CONCLUSIONS

Transition metal–fullerene complexes can show a wide variety of structures ranging from monomeric and dimeric to polymeric species. We obtained nickel-bridged fullerene polymer **1** as single crystals, allowing a first determination of the molecular and crystal structures of the metal-bridged polymer. Coordination of each nickel atom to two fullerene molecules closes fullerene cages within the polymer. In addition, polymeric chains are also densely packed in crystals to form close three-dimensional fullerene packing. Fullerenes are neutral in the polymer, and as a result, nickel atoms are also

dx.doi.org/10.1021/ic501551y | *Inorg. Chem.* 2014, 53, 11960–11965

neutral and have a diamagnetic d^{10} electron configuration. However, we suppose that the use of paramagnetic metal atoms such as cobalt(0) for the preparation of such polymers can provide promising magnetic properties. This work is now in progress. Polymer **1** obtained by us has some similarities with previously described powdered $C_{60}Pd_x$ and $C_{60}Pt_x$ polymers with x close to 1.[5a−c] Their structures can be similar. It was also shown that there is no charge transfer from zerovalent metal atoms to C_{60} in these polymers. We suppose that crystalline palladium− and platinum−fullerene polymers can be obtained using our method.

EXPERIMENTAL SECTION

Materials. Dichlorobis(trimethylphosphine)nickel(II) ($Ni^{II}\{Me_3P\}_2Cl_2$) was purchased from Aldrich, and C_{60} of 99.98% purity was purchased from MTR Ltd. *o*-Dichlorobenzene ($C_6H_4Cl_2$) was distilled over CaH_2 under reduced pressure, benzonitrile was distilled over sodium under reduced pressure, and *n*-hexane was distilled over sodium benzophenone. *N*,*N*-Dimethylformamide (DMF; Aldrich) was used as received. The solvents were degassed and stored in a glovebox. All manipulations for the synthesis of **1** were carried out in a MBraun 150B-G glovebox with a controlled atmosphere and the content of H_2O and O_2 less than 1 ppm. The crystals were stored in the glovebox and were sealed in 2 mm quartz tubes for EPR and SQUID measurements under 10^{-5} Torr. KBr pellets for the IR and UV−visible−NIR measurements were prepared in the glovebox.

Synthesis. Reduction of a stoichiometric mixture of $Ni^{II}(Me_3P)_2Cl_2$ (12 mg, 0.043 mmol) and fullerene C_{60} (30 mg, 0.042 mmol) by an excess of zinc dust (200 mg) in *o*-dichlorobenzene (16 mL) was carried out at 160 °C over 10 min. The solution was cooled to room temperature, 0.1 mL of DMF was added, and it was stirred an additional 24 h, producing a green solution. The solution was filtered in a glass tube of 46 mL volume, and *n*-hexane (26 mL) was layered on the obtained solution. Slow diffusion of hexane over 1 month yielded crystals on the wall of the tube suitable for X-ray diffraction study. The solvent was decanted from the crystals, which were washed with hexane to give black needlelike crystals of **1** in 68% yield. Platelike crystals were also formed in low yield (only about 10 platelike crystals were found) in the synthesis with DMF together with the needlelike crystals. Testing of the platelike crystals showed them to be isostructural to the needlelike crystals. The composition of the crystals was determined by X-ray diffraction as **1**.

Similarly, the synthesis of **1** was carried out with the addition of 0.1 mL of benzonitrile instead of DMF. The solution turned green, and slow mixing of the obtained solution with hexane over 1 month produced black needlelike crystals of **1**, which were isostructural to the crystal obtained with the addition of DMF.

General Procedures. UV−visible−NIR spectra were measured in KBr pellets on a PerkinElmer Lambda 1050 spectrometer in the 250−2500 nm range. Fourier transform IR spectra were obtained in KBr pellets with a PerkinElmer 1000 series spectrometer (400−7800 cm^{-1}). EPR spectra were recorded for the polycrystalline sample at room temperature with a JEOL JES-TE 200 X-band ESR spectrometer. A Quantum Design MPMS-XL SQUID magnetometer was used to measure the static magnetic susceptibility at a 100 mT magnetic field under cooling and heating conditions in the 300−1.9 K range.

Computational Details. DFT calculations by CAM-B3LYP[14] were carried out on the oligomer models of $\{Ni(PMe_3)_2\}(C_{60})_2$, $\{Ni(PMe_3)_2\}_2(C_{60})_3$, $\{Ni(PMe_3)_2\}_3(C_{60})_4$, and $\{Ni(PMe_3)_2\}_4(C_{60})_5$ from X-ray structural data. The LanL2DZ[15] and 6-31G(d,p)[16] basis sets were used for nickel and the other atoms, respectively. The stabilities of wave functions were confirmed by specifying the "Stable=Opt" keyword in the present DFT calculations. All of the computations were performed with the *Gaussian 09* program package.[17]

Crystal Data and Disorder for 1. Crystal data for **1** at 280(1) K: $C_{66}H_{18}NiP_2$, M_r = 931.45, black plate, orthorhombic, *Pbna*, a = 11.0872(19) Å, b = 19.385(3) Å, c = 16.484(3) Å, V = 3542.9(10) Å^3, Z = 4, d_{calc} = 1.746 g cm^{-3}, μ = 0.696 mm^{-1}, $F(000)$ = 1888, $2\theta_{max}$ = 50.484°, reflections measured 33186, unique reflections 4684, reflections with $I > 2\sigma(I)$ = 2463, parameters 585, restraints 716, R1 = 0.0774, wR2 = 0.2547, GOF = 1.040. The CCDC number is 1010989.

Crystal data for **1** at 100(1) K: $C_{132}H_{36}Ni_2P_4$, M_r = 931.45, black block, monoclinic, $P\ 2_1/c$, a = 19.761(5) Å, b = 19.351(5) Å, c = 19.762(5) Å, β = 111.914(5)°, V = 7011(3) Å^3, Z = 8, d_{calc} = 1.765 g cm^{-3}, μ = 0.703 mm^{-1}, $F(000)$ = 3776, $2\theta_{max}$ = 50.484°, reflections measured 60708, unique reflections 18211, reflections with $I > 2\sigma(I)$ = 8540, parameters refined 2316, restraints 5646, R1 = 0.0742, wR2 = 0.2222, GOF = 1.012. The CCDC number is 1010988.

Data collection for the crystal of **1** was carried out on a Bruker Smart Apex II CCD diffractometer with graphite-monochromated Mo Kα radiation under controlled temperature by a Japan Thermal Engineering Co. DX-CS190LD cooling system. Raw data reduction to F^2 was carried out using Bruker *SAINT*.[18] The structures were solved by the direct method and refined by the full-matrix least-squares method against F^2 using *SHELX-97*.[19] Non-hydrogen atoms were refined in the anisotropic approximation. The positions of the hydrogen atoms were included in the refinement in a riding mode. There are two orientations of C_{60} in the crystal structure of **1** at 280 K, which have the 0.608(5)/0.392(5) occupancies. There are four halves of crystallographically independent C_{60} molecules in the crystal structure of **1** at 100 K. All of them are disordered between two orientations with the 0.631(6)/0.369(6), 0.598(9)/0.402(9), 0.888(4)/0.112(4), and 0.741(5)/0.259(5) occupancies. Because of a great number of weak reflections and a great number of refined parameters, we used the DELU, ISOR, and SAME instructions to keep the parameters of fullerene cages reasonable. That results in a great number of restraints used for the refinement of the crystal structure of **1** at both 280 and 100 K.

ASSOCIATED CONTENT

Supporting Information

X-ray crystallographic data in CIF format, IR spectra, calculated models, state, total, and relative energies, calculated charges by Mulliken and natural popoulation analysis, and average charges. This material is available free of charge via the Internet at http://pubs.acs.org.

AUTHOR INFORMATION

Corresponding Author

*E-mail: konarev@icp.ac.ru.

Notes

The authors declare no competing financial interest.

ACKNOWLEDGMENTS

The work was supported by the Russian Science Foundation (Project 14-13-00028) and by JSPS Kakenhi (Grants 23225005 and 26288035). Y. N. is indebted to JGC-S SCHOLARSHIP FOUNDATION. Theoretical calculations were performed at the Research Center for Computational Science, Okazaki, Japan.

REFERENCES

(1) (a) Fagan, P. J.; Calabrese, J. C.; Malone, B. *Acc. Chem. Res.* **1992**, *25*, 134. (b) Bashilov, V. V.; Petrovskii, P. V.; Sokolov, V. I.; Lindeman, S. V.; Guzey, I. A.; Struchkov, Yu. T. *Organometallics* **1993**, *12*, 991. (c) Balch, A. L.; Catalano, V. J.; Lee, J. W.; Olmstead, M. M.; Parkin, S. R. *J. Am. Chem. Soc.* **1991**, *113*, 8953. (d) Shevelev, Yu. A.; Markin, G. V.; Konarev, D. V.; Fukin, G. K.; Lopatin, M. A.; Shavyrin, A. S.; Baranov, E. V.; Lyubovskaya, R. N.; Domrachev, G. A. *Dokl. Chem.* **2007**, *412*, 18. (e) Bengough, M.; Thompson, D. M.; Baird, M. C.;

Enright, G. D. *Organometallics* **1999**, *18*, 2950. (f) Balch, A. L.; Olmstead, M. M. *Chem. Rev.* **1998**, *98*, 2123.
(2) (a) Fagan, P. J.; Calabrese, J. C.; Malone, B. *J. Am. Chem. Soc.* **1991**, *113*, 9408. (b) Balch, A. L.; Lee, J. W.; Noll, B. C.; Olmstead, M. M. *J. Am. Chem. Soc.* **1992**, *114*, 10984.
(3) (a) Jin, X.; Xie, X.; Tang, K. *Chem. Commun.* **2002**, 750. (b) Konarev, D. V.; Troyanov, S. I.; Nakano, Y.; Ustimenko, K. A.; Otsuka, A.; Yamochi, H.; Saito, G.; Lyubovskaya, R. N. *Organometallics* **2013**, *32*, 4038. (c) Konarev, D. V.; Troyanov, S. I.; Nakano, Y.; Otsuka, A.; Yamochi, H.; Saito, G.; Lyubovskaya, R. N. *Dalton Trans.* **2014**, DOI: 10.1039/C4DT02161D.
(4) (a) Lee, G.; Cho, Y.-J.; Park, B. K.; Lee, K.; Park, J. T. *J. Am. Chem. Soc.* **2003**, *125*, 13920. (b) Lee, K.; Song, H.; Kim, B.; Park, J. T.; Park, S.; Choi, M.-G. *J. Am. Chem. Soc.* **2002**, *124*, 2872.
(5) (a) Nagashima, H.; Nakaota, A.; Saito, Y.; Kato, M.; Kawanishi, T.; Itoh, K. *J. Chem. Soc., Chem. Commun.* **1992**, 377. (b) Nagashima, H.; Nakaoka, A.; Tajima, S.; Saito, Y.; Itoh, K. *Chem. Lett.* **1992**, 1361. (c) Nagashima, H.; Kato, Y.; Yamaguchi, H.; Kimura, E.; Kawanishi, T.; Kato, M.; Saito, Y.; Haga, M.; Itoh, K. *Chem. Lett.* **1994**, 1207. (d) Hayashi, A.; de Bettencourt-Dias, A.; Winkler, K.; Balch, A. L. *J. Mater. Chem.* **2002**, *12*, 2116. (e) Grodzka, E.; Pięta, P.; Dluzewski, P.; Kutner, W.; Winkler, K. *Electrochim. Acta* **2009**, *54*, 5621. (f) Pieta, P.; Grodzka, E.; Winkler, K.; Warczak, M.; Sadkowski, A.; Zukowska, G. Z.; Venukadasula, G. M.; D'Souza, F.; Kutner, W. *J. Phys. Chem. B* **2009**, *113*, 6682. (g) Balch, A. L.; Costa, D. A.; Winkler, K. *J. Am. Chem. Soc.* **1998**, *120*, 9614. (h) Winkler, K.; Balch, A. L. *C. R. Chim.* **2006**, *9*, 928. (i) Ginwalla, A. S.; Balch, A. L.; Kauzlarich, S. M.; Irons, S. H.; Klavins, P.; Shelton, R. N. *Chem. Mater.* **1997**, *9*, 278.
(6) (a) Konarev, D. V.; Khasanov, S. S.; Yudanova, E. I.; Lyubovskaya, R. N. *Eur. J. Inorg. Chem.* **2011**, 816. (b) Konarev, D. V.; Simonov, S. V.; Khasanov, S. S.; Lyubovskaya, R. N. *Dalton Trans.* **2011**, *40*, 9176. (c) Konarev, D. V.; Troyanov, S. I.; Khasanov, S. S.; Lyubovskaya, R. N. *J. Coord. Chem.* **2013**, *66*, 4178. (d) Konarev, D. V.; Khasanov, S. S.; Troyanov, S. I.; Nakano, Y.; Ustimenko, K. A.; Otsuka, A.; Yamochi, H.; Saito, G.; Lyubovskaya, R. N. *Inorg. Chem.* **2013**, *52*, 13934.
(7) Litvinov, A. L.; Konarev, D. V.; Yudanova, E. I.; Kaplunov, M. G.; Lyubovskaya, R. N. *Russ. Chem. Bull.* **2002**, *51*, 2003.
(8) Picher, T.; Winkler, R.; Kuzmany, H. *Phys. Rev. B* **1994**, *49*, 15879.
(9) (a) Reed, C. A.; Bolskar, R. D. *Chem. Rev.* **2000**, *100*, 1075. (b) Konarev, D. V.; Lyubovskaya, R. N. *Russ. Chem. Rev.* **2012**, *81*, 336.
(10) Stephens, P. W.; Bortel, G.; Faigel, G.; Tegze, M.; Jánossy, A.; Pekker, S.; Oszlanyi, G.; Forró, L. *Nature* **1994**, *370*, 636.
(11) (a) Izuoka, A.; Tachikawa, T.; Sugawara, T.; Suzuki, Y.; Konno, M.; Saito, Y.; Shinohara, H. *J. Chem. Soc., Chem. Commum.* **1992**, 1472. (b) Konarev, D. V.; Neretin, I. S.; Slovokhotov, Yu. L.; Yudanova, E. I.; Drichko, N. V.; Shulga, Yu. M.; Tarasov, B. P.; Gumanov, L. L.; Batsanov, A. S.; Howard, J. A. K.; Lyubovskaya, R. N. *Chem.—Eur. J.* **2001**, *7*, 2605. (c) Narimbetov, B.; Kobayashi, H.; Tokumoto, M.; Omerzu, A.; Mihailovic, D. *Chem. Commun.* **1999**, 1511.
(12) (a) Heiney, P. A.; Fischer, J. E.; McGhie, A. R.; Romanov, W. J.; Denenstein, A. M.; McCauley, J. P., Jr.; Smith, A. B.; Cox, D. E. *Phys. Rev. Lett.* **1991**, *66*, 2911. (b) O'Neil, A.; Wilson, C.; Webster, J. M.; Allison, F. J.; Howard, J. A. K.; Poliakoff, M. *Angew. Chem., Int. Ed.* **2002**, *41*, 3796.
(13) Heiney, P. A.; Fischer, J. E.; McGhie, A. R.; Romanov, W. J.; Denenstein, A. M.; McCauley, J. P., Jr.; Smith, A. B., III; Cox, D. E. *Phys. Rev. Lett.* **1991**, *67*, 1468.
(14) (a) Yanai, T.; Tew, D.; Handy, N. *Chem. Phys. Lett.* **2004**, *393*, 51. (b) Peach, M. J. G.; Benfield, P.; Helgaker, T.; Tozer, D. J. *J. Chem. Phys.* **2008**, *128*, 044118.
(15) (a) Hay, P. J.; Wadt, W. R. *J. Chem. Phys.* **1985**, *82*, 270. (b) Wadt, W. R.; Hay, P. J. *J. Chem. Phys.* **1985**, *82*, 284. (c) Hay, P. J.; Wadt, W. R. *J. Chem. Phys.* **1985**, *82*, 299.
(16) (a) Hehre, W. J.; Ditchfield, R.; Pople, J. A. *J. Chem. Phys.* **1972**, *56*, 2257. (b) Hariharan, P. C.; Pople, J. A. *Mol. Phys.* **1974**, *27*, 209. (c) Hariharan, P. C.; Pople, J. A. *Theor. Chim. Acta* **1973**, *28*, 213. (d) Francl, M. M.; Pietro, W. J.; Hehre, W. J.; Binkley, J. S.; Gordon, M. S.; DeFrees, D. J.; Pople, J. A. *J. Chem. Phys.* **1982**, *77*, 3654.
(17) Frisch, M. J.; Trucks, G. W.; Schlegel, H. B.; Scuseria, G. E.; Robb, M. A.; Cheeseman, J. R.; Scalmani, G.; Barone, V.; Mennucci, B.; Petersson, G. A.; Nakatsuji, H.; Caricato, M.; Li, X.; Hratchian, H. P.; Izmaylov, A. F.; Bloino, J.; Zheng, G.; Sonnenberg, J. L.; Hada, M.; Ehara, M.; Toyota, K.; Fukuda, R.; Hasegawa, J.; Ishida, M.; Nakajima, T.; Honda, Y.; Kitao, O.; Nakai, H.; Vreven, T.; Montgomery, J. A., Jr.; Peralta, J. E.; Ogliaro, F.; Bearpark, M.; Heyd, J. J.; Brothers, E.; Kudin, K. N.; Staroverov, V. N.; Keith, T.; Kobayashi, R.; Normand, J.; Raghavachari, K.; Rendell, A.; Burant, J. C.; Iyengar, S. S.; Tomasi, J.; Cossi, M.; Rega, N.; Millam, J. M.; Klene, M.; Knox, J. E.; Cross, J. B.; Bakken, V.; Adamo, C.; Jaramillo, J.; Gomperts, R.; Stratmann, R. E.; Yazyev, O.; Austin, A. J.; Cammi, R.; Pomelli, C.; Ochterski, J. W.; Martin, R. L.; Morokuma, K.; Zakrzewski, V. G.; Voth, G. A.; Salvador, P.; Dannenberg, J. J.; Dapprich, S.; Daniels, A. D.; Farkas, O.; Foresman, J. B.; Ortiz, J. V.; Cioslowski, J.; Fox, D. J. *Gaussian 09*, revision D.01; Gaussian, Inc.: Wallingford, CT, 2013.
(18) *SAINT*; Bruker Analytical X-ray Systems: Madison, WI, 1999.
(19) Sheldrick, G. M. *Acta Crystallogr., Sect. A* **2008**, *64*, 112.